Structural Engineering and Mechanics, *Vol. 55, No. 1 (2015) 79-92*
DOI: http://dx.doi.org/10.12989/sem.2015.55.1.079

Free vibration analysis of damaged composite beams

Yusuf Cunedioglu*[1] and Bertan Beylergil[2]

[1]*Faculty of Engineering, Mechanical Engineering Department, Nigde University, 51245, Campus, Nigde, Turkey*
[2]*Faculty of Engineering, Mechanical Engineering Department, Izmir Institute of Technology, 35437, Gulbahce Campus, Izmir, Turkey*

(Received September 17, 2014, Revised January 14, 2015, Accepted April 4, 2015)

Abstract. In this study, free vibration analyses of symmetric laminated cantilever and simply supported damaged composite beams are investigated by using finite element method (FEM). Free vibration responses of damaged beams are examined using Euler Bernoulli beam and classical lamination theories. A computer code is developed by using MATLAB software to determine the natural frequencies of a damaged beam. The local damage zone is assumed to be on the surface lamina of the beam by broken fibers after impact. The damaged zone is modeled as a unidirectional discontinuous lamina with 0^o orientations in this study. Fiber volume fraction (v_f), fiber aspect ratio (L_f/d_f), damage length (L_D) and its location (λ/L), fiber orientation and stacking sequence parameters effects on natural frequencies are investigated. These parameters are affected the natural frequency values significantly.

Keywords: fiber reinforced composites; finite element method (FEM); structural design; vibration/ vibration control

1. Introduction

Fiber reinforced composite materials are being increasingly used in aircraft, spacecraft constructions, automotive industry and in civil engineering applications due to their high stiffness to weight ratios. If a traditional engineering material, steel or aluminum, experiences low velocity impact, the energy is typically absorbed through plastic deformation. Although this deformation is permanent, it usually does not significantly reduce the load carrying capability of the structure (Bradshaw *et al*. 1972). However, this is not true for fiber reinforced composites due to the brittle nature of the epoxy matrix and low plastic deformation capability of the fibers. Three failure modes can be observed in fiber reinforced composites caused by low-velocity impact; (i) matrix cracking, (ii) delamination, and (iii) fiber failure (Lagace and Wolf 1993, Choi and Chang 1991, Cantwell and Morton 1990, Cantwell and Morton 1991). Delamination may cause stiffness reduction and sudden failure of the structure. The reduction in stiffness also affects the vibration characteristics of the composite structure. Therefore, dynamic behavior of composite structures must be taken into account in design. In the absence of analytical solutions, dynamic responses of

*Corresponding author, Ph.D. Student, E-mail: ycunedioglu@nigde.edu.tr

http://www.techno-press.org/?journal=sem&subpage=8 ISSN: 1225-4568 (Print), 1598-6217 (Online)

structural systems are calculated by computational methods, finite element methods (FEM) have been widely used.

Sun and Chen (1985) performed the dynamic analysis of laminated plates under impact loading by using three-dimensional finite element method. Cairns and Lagace (1989) investigated the effect of different parameters on the impact behavior of laminated composite plates. Chun and Kassegne (2005) studied the response of graphite/epoxy laminated composite non-prismatic folded plates subjected to impact loads by using the higher-order shear deformation theory. Tiberkak *et al*. (2008) also investigated fiber-reinforced composite plates subjected to low velocity impact, by the use of finite element analysis. Setoodeh *et al*. (2009) analyzed a three-dimensional elasticity based approach coupled with layer-wise laminated plate theory employed to conduct low velocity impact analysis of general fiber reinforced laminated composite plates, with a finite element computation algorithm. Aydogdu (2014) used the Ritz method to determine natural frequencies of aligned single walled carbon nanotube (CNT) reinforced composite beams. As previously mentioned, the effect of impact loading on dynamic response of composite beams has engaged the attention of scientists for many years and it is not a new concept; however, local damage zone is identified by broken fibers on the surface lamina of the beam. It is assumed that continuous fibers are converted into unidirectional discontinuous fibers (0^o) after impact. This modeling approach has not been studied in literature. Free vibration characteristics of the symmetric laminated composite beams (healthy/damaged) are investigated. The natural frequencies for the first three flexural modes of both the healthy and damaged beams are calculated. The effects of fiber volume fraction (v_f), fiber aspect ratio (L_f/d_f), damage length (L_D) and its location (λ/L), fiber orientation and stacking sequence on the natural frequencies are also investigated for both cantilever and simply supported boundary condition.

2. Finite element analysis of laminated composite beams

Laminated composite beams are generally made of multiple layers. In that case, to compute the stiffness matrix of symmetrically laminated composite beams the classical laminated plate theory (CLPT) is used. The classical plate theory constitutive equations for symmetric laminates, in the absence of in plane forces, are given by the following equations (Reddy 1992)

$$\begin{Bmatrix} M_{xx} \\ M_{yy} \\ M_{xy} \end{Bmatrix} = -\begin{bmatrix} D_{11} & D_{12} & D_{16} \\ D_{12} & D_{22} & D_{26} \\ D_{16} & D_{26} & D_{66} \end{bmatrix} \begin{Bmatrix} \dfrac{\partial^2 w_0}{\partial x^2} \\ \dfrac{\partial^2 w_0}{\partial y^2} \\ 2\dfrac{\partial^2 w_0}{\partial x \partial y} \end{Bmatrix} \tag{1}$$

or, in inverse form

$$\begin{Bmatrix} \dfrac{\partial^2 w_0}{\partial x^2} \\ \dfrac{\partial^2 w_0}{\partial y^2} \\ 2\dfrac{\partial^2 w_0}{\partial x \partial y} \end{Bmatrix} = -\begin{bmatrix} D_{11}^* & D_{12}^* & D_{16}^* \\ D_{12}^* & D_{22}^* & D_{26}^* \\ D_{16}^* & D_{26}^* & D_{66}^* \end{bmatrix} \begin{Bmatrix} M_{xx} \\ M_{yy} \\ M_{xy} \end{Bmatrix} \tag{2}$$

where D_{ij}^{*} denote the elements of the inverse matrix of D_{ij}. The laminated composite beam is assumed be long enough so that the effects of the Poisson ratio and shear coupling on the deflection is negligible. In deriving the laminated beam theory it is assumed that

$$M_{yy} = M_{xy} = 0 \tag{3}$$

Eq. (1) can be rewritten as

$$\frac{\partial^2 w_0}{\partial x^2} = -D_{11}^{*} M_{xx} \tag{4}$$

$$M = bM_{xx}\,,\quad E_{xx} = \frac{12}{h^3 D_{11}^{*}} = \frac{b}{I_{yy} D_{11}^{*}}\,,\quad E_{xx} I_{yy} = \frac{b}{D_{11}^{*}}\,,\quad I_{yy} = \frac{bh^3}{12} \tag{5}$$

where b is the width and h is the thickness of the composite beam. In the finite element formulation, Langrange interpolation functions are used. Derivation of the stiffness and mass matrices of an element are based on the energy approach (Kiral 2009). For free vibration of a beam, the eigenvalue problem is defined in the following equation (Kumar *et al*. 2011)

$$\left([K] - \omega^2 [M]\right)\left\{\bar{d}\right\} = 0 \tag{6}$$

where ω is the angular natural frequency in radians per second, $\{d\}$ is the mode shape, $[K]$ is the stiffness matrix and $[M]$ is the mass matrix of the beam system.

3. 0^o lamina with discontinuous fibers

Computation of elastic properties of a unidirectional discontinuous fiber 0^o lamina is derived from the Halpin- Tsai equations with the following assumptions (Kaw 2006);

- Fiber cross sectional area is circular.
- Fibers are arranged in the form of square array.
- Fibers are uniformly distributed throughout the matrix phase.
- Perfect bonding assumed between the fibers and the matrix.
- Matrix does not have any voids.

Elastic properties of a unidirectional discontinuous fiber 0^o lamina are calculated using the following equations (Kaw 2006)

$$E_1 = \frac{1 + 2\left(l_f \big/ d_f\right)\eta_L \upsilon_f}{1 - \eta_L \upsilon_f} E_m \tag{7}$$

$$E_2 = \frac{1 + 2\eta_T \upsilon_f}{1 - \eta_T \upsilon_f} E_m \tag{8}$$

$$G_{12} = G_{21} = \frac{1 + \eta_G \upsilon_f}{1 - \eta_G \upsilon_f} G_m \tag{9}$$

$$\nu_{12} = \nu_f \upsilon_f + \nu_m \upsilon_m \tag{10}$$

$$\upsilon_{21} = \frac{E_2}{E_1}\upsilon_{12} \tag{11}$$

where indices *m* and *f* denote matrix and fiber, respectively. *E*, *G*, and *v* are the modulus of elasticity, modulus of rigidity, and the Poisson's ratio respectively. The terms in Eqs. (7)-(9) can be calculated as follows (Kaw 2006)

$$\eta_L = \frac{\left(E_f/E_m\right)-1}{\left(E_f/E_m\right)+2\left(l_f/d_f\right)} \tag{12}$$

$$\eta_T = \frac{\left(E_f/E_m\right)-1}{\left(E_f/E_m\right)+2} \tag{13}$$

$$\eta_G = \frac{\left(G_f/G_m\right)-1}{\left(G_f/G_m\right)+1} \tag{14}$$

Fiber aspect ratio, defined as the ratio of average fiber length L_f to fiber diameter d_f, has a significant effect on the longitudinal modulus E_1. On the other hand, the transverse modulus E_2 is not affected by the fiber aspect ratio. Moreover, the longitudinal modulus E_1 for a discontinuous fiber 0^o lamina is always less than that for a continuous fiber 0^o lamina.

4. Numerical verification

In this study, a finite element code is generated by using MATLAB program. 2D beam elements (2 DOF per node) are used for the numerical modeling. The FE model is validated by comparing with results from the literature for a four-layer symmetric cross-ply $[0/90]_s$. Numerical analyses are carried out for the following composite beam data: length (*L*) 0.381 m, thickness (*h*) 0.0254 m, width (*b*) 0.0254 m. The material properties of graphite/epoxy composite are: longitudinal modulus E_1=144.80 GPa, transverse modulus E_2=9.65 GPa, shear modulus G_{23}=3.45 GPa, G_{12}=G_{13}=4.14 GPa, Poisson ratio (v)=0.3 density ρ=1389 kg/m^3. The non-dimensional natural frequency is given as (Cunedioglu 2011, Cevik 2010)

$$\bar{\omega} = \omega L^2 \sqrt{\frac{\rho}{E_1 h^2}} \tag{15}$$

where $\bar{\omega}$ is the non-dimensional natural frequency. The analytical solution of the cantilever composite beam for the first mode is given by the following equation (Harris 2002)

$$\omega = \frac{\left(1.875\right)^2}{L^2}\sqrt{\frac{EI}{E_1 h^2}} \tag{16}$$

Table 1 Non-dimensional fundamental frequencies of a $[0/90]_s$ Graphite/Epoxy cantilever composite beam

Numayr *et al.*(2006)	Yildirim and Kiral (2000)	Chen *et al.* (2003)	Present study	Analytical
0.95582	0.9215	0.9149	0.95394	0.95383

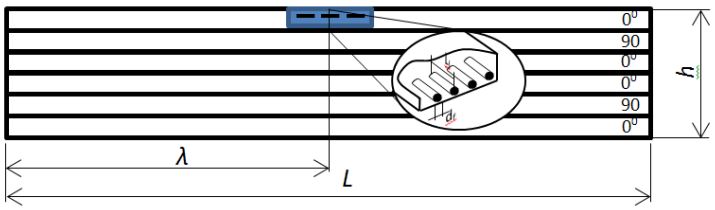

Fig. 1 The geometrical characteristics of the composite beam

Non-dimensional fundamental frequencies of graphite-epoxy composite beam are given in Table 1. It is seen that the results of the developed finite element beam model show good agreement with the analytical and finite element results given in the literature. After the validation step, the model is extended to study the following problem.

5. Problem statement

The aim of this study is to investigate free vibration characteristics of the symmetric graphite/epoxy laminated composite beams (healthy or damaged). The damaged composite beams are modeled by assuming the following condition: the continuous fibers on the surface lamina of the beam are converted into unidirectional discontinuous fibers (0^o) after impact. The material properties of the graphite fiber-reinforced polyamide composite, in terms of fibers and matrix, identified by the indices *f* and *m*, respectively, are given as follows (Kisa 2004);

Modulus of elasticity: E_f=275.6 MPa, E_m=2.756 MPa

Shear modulus: G_f=114.8 MPa, G_m=1.036 MPa

Poisson ratio: υ_f=0.2; υ_m=0.33

Density: ρ_f=1900 kg/m^3, ρ_m=1600 kg/m^3

Fig. 1 shows the geometrical characteristics of the beam. The length (L), height (h) and width (b) of the composite beam are chosen as 1.2 m, 0.012 m and 0.06 m; respectively. Each lamina contains thirty fibers and the fiber orientation is $[0/90/0]_s$.

For L_d = 120 mm, 240, 360 and 480 mm; 6, 12, 18 and 24 elements are used in the damaged zone; respectively. Two boundary conditions are considered; cantilever and simply supported. Converge studies are conducted to choose best finite element mesh (Table 2) and the authors decided to use sixty elements for each model. The damage length (L_d) is varied as 120, 240, 360 and 480 mm. Fiber aspect ratio (L_f/d_f) is changed from 1 to 60 by an increment of 15. The calculated fiber diameters for v_f=0.4, 0.5, 0.6 and 0.7 are 0.001427, 0.001596, 0.001748 and 0.001888 m; respectively.

The mechanical properties of laminated composite beam are calculated by using following formulas (Kisa 2004)

Table 2 Results of converge studies*

	Natural Frequency (Hz)	20 elements	30 elements	40 elements	50 elements	60 elements
Cantilever boundary condition	1st mode	9.4521	9.4521	9.4521	9.4521	9.4521
	2nd mode	59.2355	59.2354	59.2354	59.2354	59.2354
	3rd mode	165.8635	165.8613	165.8610	165.8609	165.8608
	Natural Frequency (Hz)	**20 elements**	**30 elements**	**40 elements**	**50 elements**	**60 elements**
Simply-supported boundary condition	1st mode	26.5325	26.5324	26.5324	26.5324	26.5324
	2nd mode	106.1306	106.1301	106.1300	106.1299	106.1299
	3rd mode	238.8005	238.7940	238.7929	238.7926	238.7925

(*) Fiber volume fraction v_f=0.4 and lamination sequence: $[0/90/0]_s$

$$\rho = \rho_f v_f + \rho_m (1 - v_f) \tag{17}$$

$$E_1 = E_f v_f + E_m \left(1 - v_f\right) \tag{18}$$

$$E_2 = E_m \left[\frac{E_f + E_m + \left(E_f - E_m\right) v_f}{E_f + E_m - \left(E_f - E_m\right) v_f} \right] \tag{19}$$

$$\upsilon_{12} = \upsilon_f v_f + \upsilon_m \left(1 - v_f\right) \tag{20}$$

$$\upsilon_{23} = \upsilon_f v_f + \upsilon_m \left(1 - v_f\right) \left[\frac{1 + \upsilon_m - \upsilon_{12} E_m / E_1}{1 - \upsilon_m{}^2 + \upsilon_m \upsilon_{12} E_m / E_1} \right] \tag{21}$$

$$G_{23} = \frac{E_2}{2(1 + \upsilon_{23})} \tag{22}$$

6. Results and discussion

Fig. 2 shows variation of the first three natural frequency with respect to the fiber aspect ratio (L_f/d_f) and fiber volume fraction (v_f). The damage length and damage location are kept constant as 0.12 m and 0.5 respectively. It is seen that the natural frequency for every fiber aspect ratio increases with the respect to an increase in the fiber volume fraction and a higher aspect ratio leads to a higher natural frequency. This is because natural frequency is a function of elastic moduli which increases with the increase of fiber aspect ratio and volume fraction. For cantilever boundary condition, this increase is uniform for all modes but the second mode natural frequency

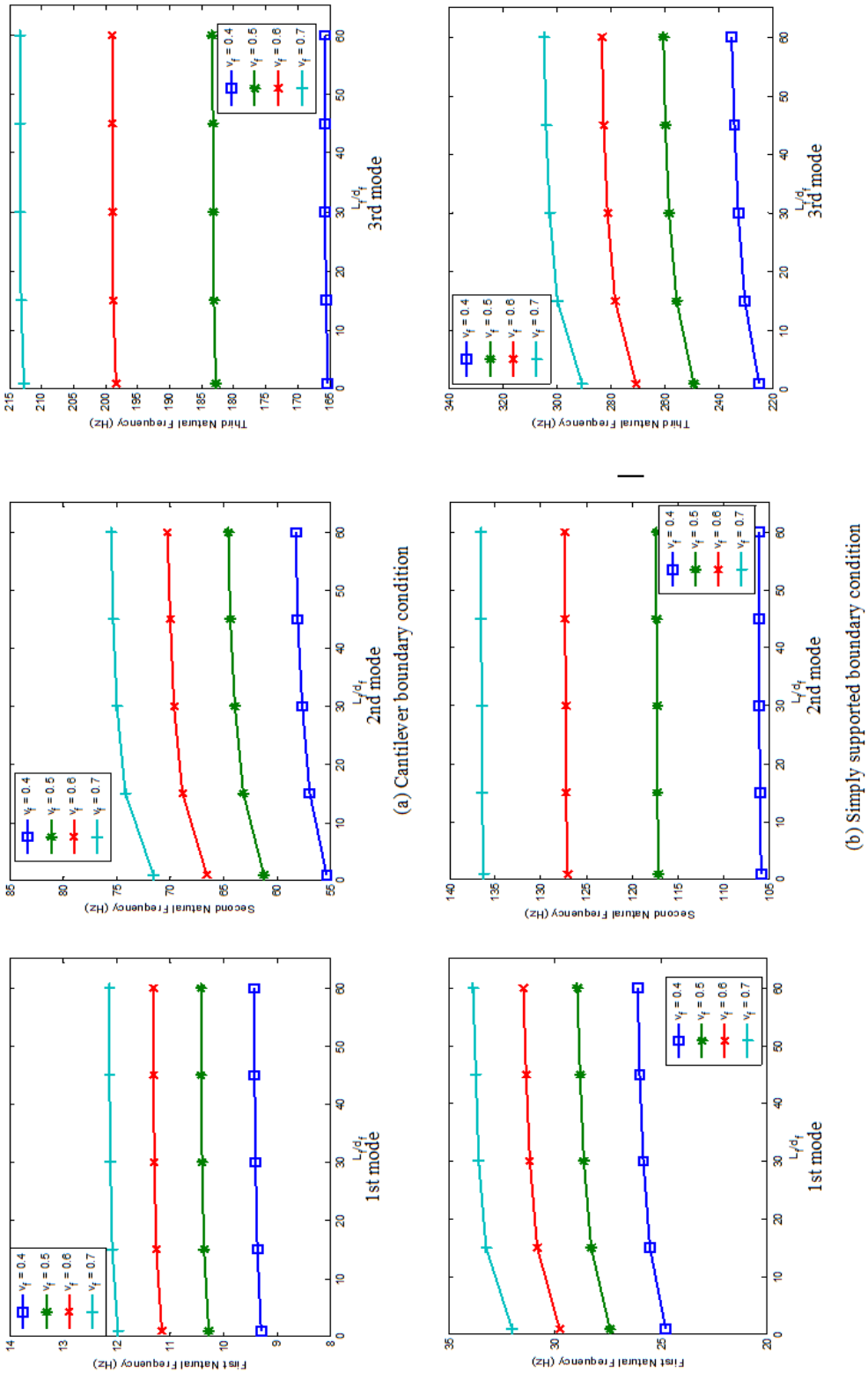

Fig. 2 Variation of the first three natural frequency with respect to the fiber aspect ratio (L_f/d_f) and fiber volume fraction (v_f) for $[0/90/0]_s$, L_d=0.12 m, and λ/L=0.5; (a) cantilever and (b) simply supported boundary condition

Table 3 The first three natural frequency of a $[0/90/0]_s$ Graphite/Epoxy cantilever composite beam (v_f=0.4, λ/L=0.5)

L_f/d_f	ω_1 (Hz)	ω_2 (Hz)	ω_3 (Hz)
1	9.288	55.315	165.228
15	9.359	56.915	165.506
30	9.389	57.621	165.620
45	9.404	57.998	165.678
60	9.413	58.233	165.714
84.09*	9.452	59.236	165.860
Healthy beam	*9.452*	*59.235*	*165.860*

(*) For this value, L_f=120 mm.

being affected more than others. For simply supported condition, the natural frequency values increase with the increase of fibers aspect ratio and fiber volume fraction (v_f). The second mode is slightly affected. Damage zone becomes unidirectional as fiber aspect ratio increases. The validation of this statement is shown in Table 3 for $[0/90/0]_s$ cantilever beam.

Variation of the first three natural frequencies with respect to the fiber aspect ratio (L_f/d_f) and damage length (L_d) is shown in Fig. 3. Fiber volume fraction v_f=0.4 and damage location λ/L=0.5 are kept constant. It is seen that the natural frequency decrease with the increase of damage length for all modes but for cantilever boundary condition the third mode is not affected significantly when damage length (L_d) 120 mm. Same trend is observed for second mode simply supported boundary condition.

Fig. 4 shows the variation of the first three natural frequency with respect to the fiber aspect ratio (L_f/d_f) and damage location (λ/L). L_d=0.12 m, v_f=0.4 are kept constant. For cantilever boundary condition, the first mode frequency values continuously increase when the damage zone is become closer to the free end of the beam (λ/L increases). The increase of natural frequency is well detected as λ/L increases from 0.55 to 0.75 then the frequency values are become less affected by damage location. The frequencies of the second and third modes show different behavior in this case so that the second mode natural frequencies tend to increase gradually until λ/L=0.25 then the frequency values decrease almost linearly until λ/L ratio is 0.55. After that the values start to increase with the increase of λ/L ratio. The third mode response is similar to the previous mode. It is worth noticing that the minimum second and third mode natural frequency are observed as the λ/L ratio reaches to 0.55 and 0.75 respectively for all L_f/d_f ratios. For simply-supported boundary condition, the first mode natural frequency values decrease with the increase of λ/L ratio until this ratio reaches to 0.5. The minimum second mode natural frequency values are observed when λ/L ratio is 0.25 and 0.75 and the minimum third mode natural frequency values are observed when λ/L ratio is 0.15 and 0.85 for all L_f/d_f ratios.

Variation of the first three natural frequency with respect to different stacking sequence and damage location (λ/L) for L_d=0.12 m, v_f=0.4 is shown in Fig. 5. For both cantilever and simply-supported boundary condition, as expected, the maximum natural frequencies was obtained for $[0]_{3s}$ composite beam because the beam is stiffer than the others. For cantilever boundary condition, it is seen that the increase of damage location λ/L cause a noticeable increase in the first mode natural frequencies. For both boundary conditions, the second and third mode natural frequencies are also affected by stacking sequence but in a different manner so that the variation of these

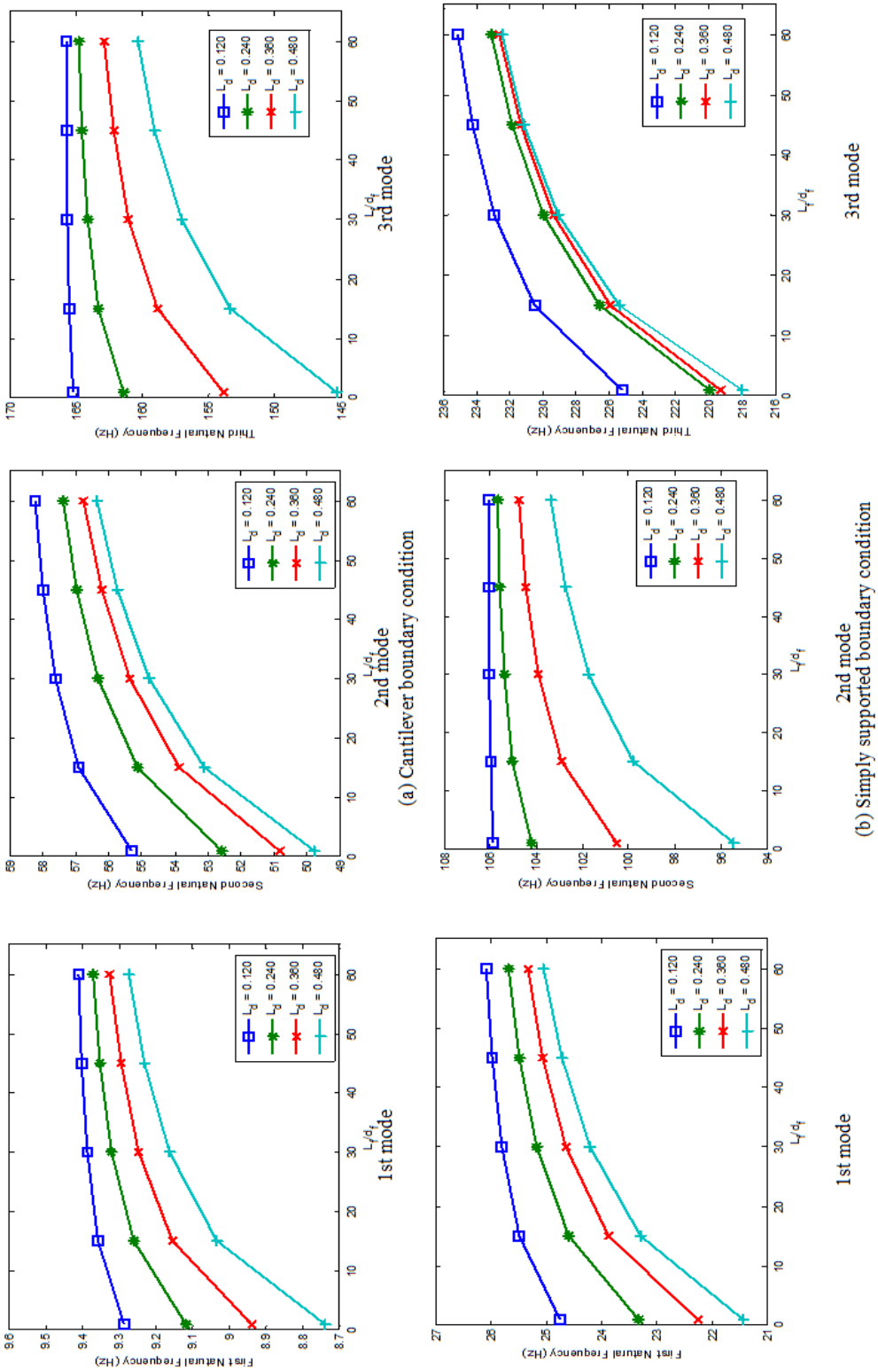

Fig. 3 Variation of the first three natural frequency with respect to the fiber aspect ratio (L_f/d_f) and damage length (L_d) for $[0/90/0]_s$ beam, v_f=0.4 and λ/L=0.5; (a) cantilever and (b) simply supported boundary condition

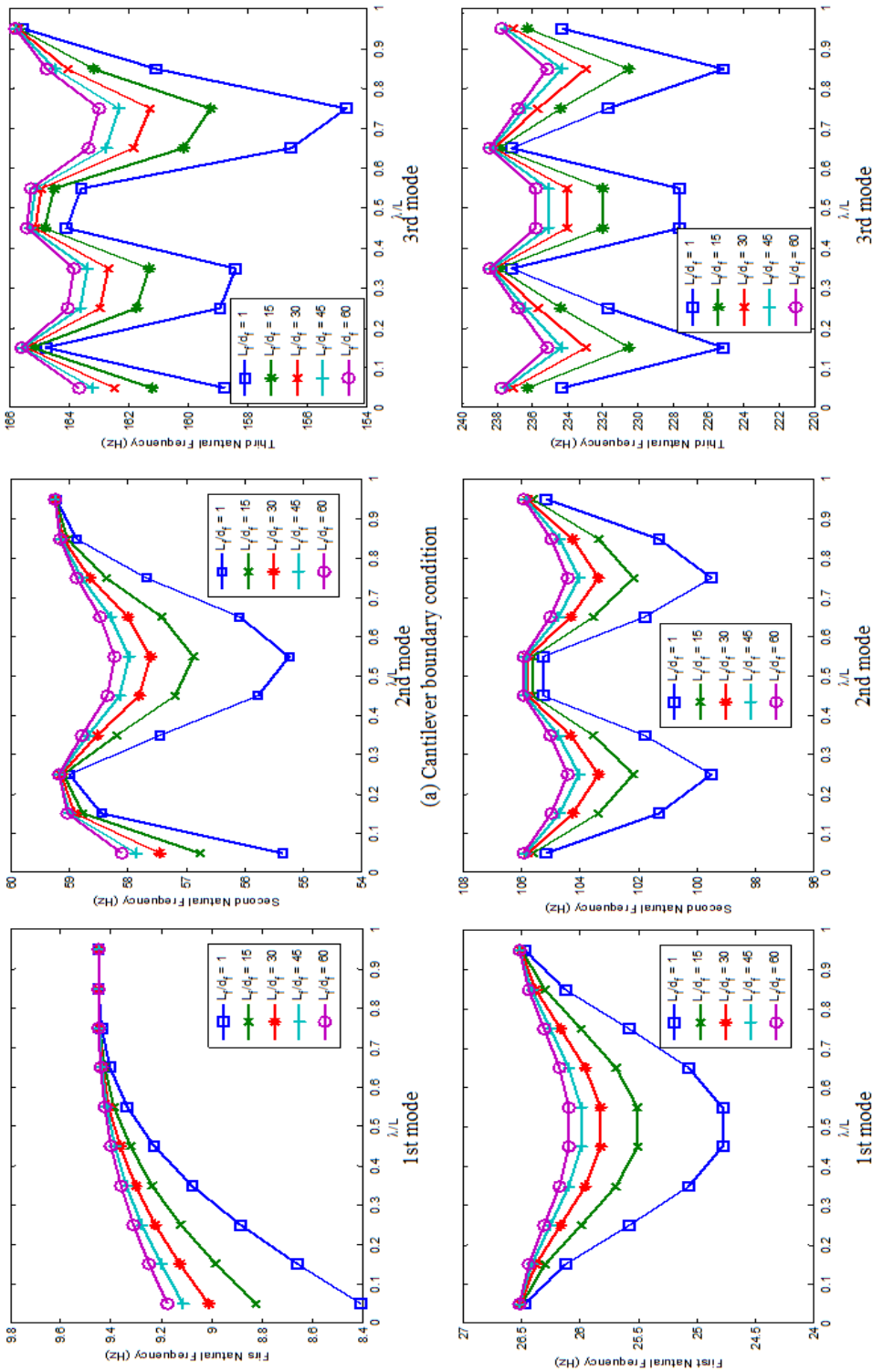

Fig. 4 Variation of the first three natural frequency with respect to the fiber aspect ratio (L_f/d_f) and damage location (λ/L) for $[0/90/0]_s$ beam, L_d=0.12 m, v_f=0.4; (a) cantilever and (b) simply supported boundary condition

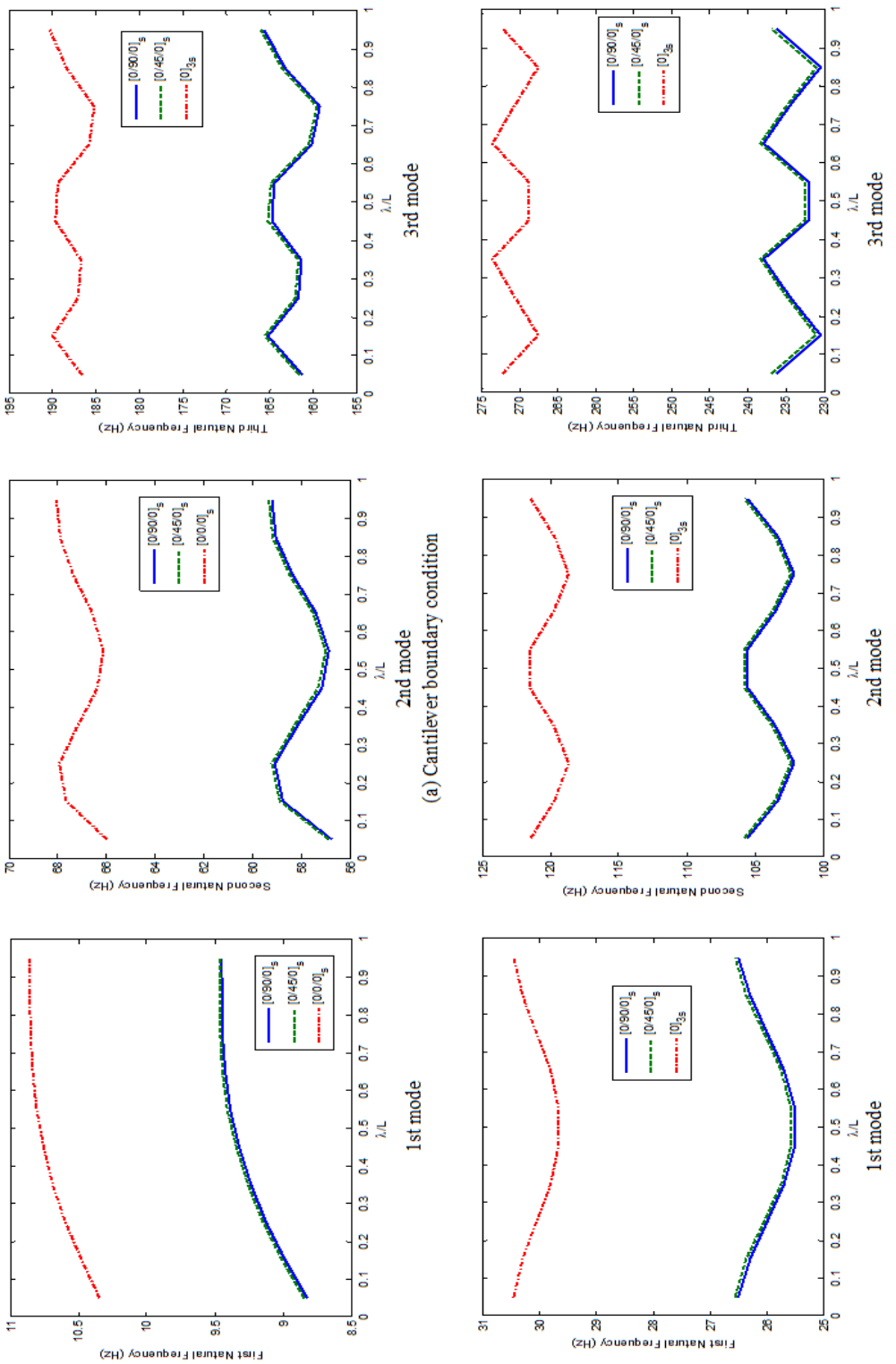

Fig. 5 Variation of the first three natural frequency with respect to the stacking sequence and damage location (λ/L) of the beam for L_d =0.12m, v_f=0.4; (a) cantilever and (b) simply supported boundary condition

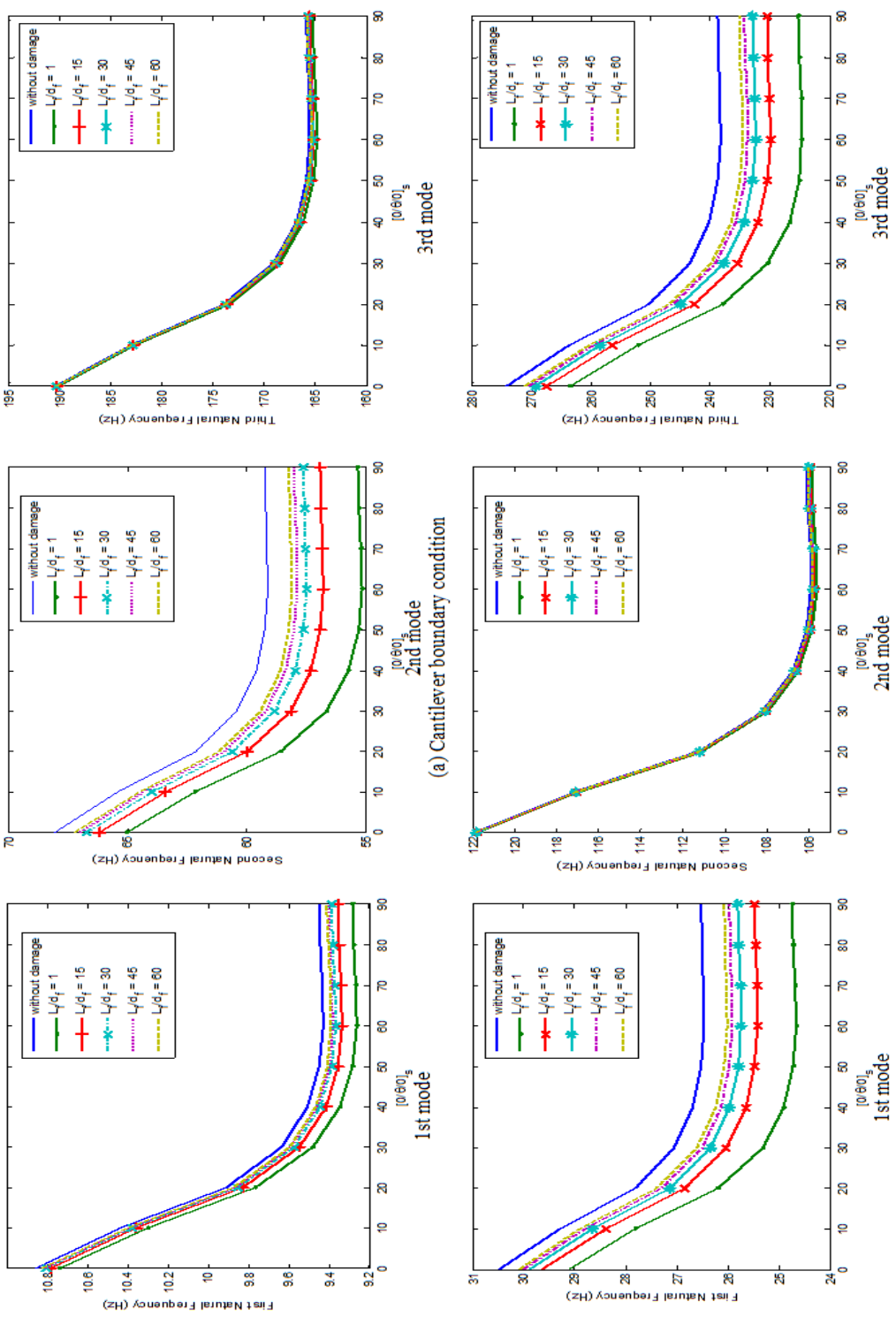

Fig. 6 Variation of the first three natural frequency of the clamped healthy/damaged beam as a function of θ and fiber aspect ratio (L_f/d_f) for L_d = 0.12 m, v_f = 0.4; (a) cantilever and (b) simply supported boundary condition

modes shows a series of maxima and minima respectively with the increase of damage location. For simply supported boundary condition, the first mode natural frequency decreases until the damage location is 0.5 then the frequency values begin to increase. The minimum frequency values are observed for the beam with $[0/90/0]_s$ stacking sequence for all cases.

Fig. 6 shows variation of the first three natural frequency of the healthy/damaged beam as a function of θ and fiber aspect ratio (L_f/d_f) for L_d=0.12 m, v_f=0.4. For both cantilever and simply supported boundary condition, it is noteworthy that the increase of the angle of θ causes a reduction in natural frequency values. When the angle of θ is higher than 60^o, a small increase is observed for all cases. It is also seen that the healthy beam has the highest frequency values for all modes. As seen in the figure, second mode for cantilever boundary condition is not affected significantly by fiber aspect ratio and the same tendency is observed for third mode for simply supported boundary condition.

7. Conclusions

In this study, free vibration characteristics of the symmetric laminated composite beams (healthy/damaged) are investigated. A new local damage model is proposed by broken fibers on the upper surface lamina of the beam. It is assumed that continuous fibers are broken into unidirectional discontinuous fibers (0^o) after impact. The modal frequencies for the first three flexural modes of both the healthy and the damaged beams are calculated. The following conclusions can be drawn from the results:

• The natural frequency values increase with the increase of fibers aspect ratio (L_f/d_f) and fiber volume fraction (v_f).

• The increase in damage location (λ/L) causes a noticeable increase in the first mode natural frequency.

• The increase of the angle of θ causes a reduction in natural frequency values.

References

Aydogdu, M. (2014), "On the vibration of aligned carbon nanotube reinforced composite beams", *Adv. Nano Res.*, **2**(4), 199-210.

Bradshaw, F.J., Dorey, G. and Sidey, G.R. (1972), "Impact resistance of carbon reinforced plastics", *Proceedings of the Designing to Avoid Mechanical Failure Conference*, 8-10.

Cairns, D.S. and Lagace, P.A. (1989), "Transient response of graphite/epoxy and kevlar/epoxy laminates subjected to impact", *AIAA J.*, **27**(11), 1590-1596.

Cantwell, W.J. and Morton, J. (1990), "Impact perforation of carbon fibre reinforced plastic", *Compos. Sci. Technol.*, **38**, 119-141.

Cantwell, W.J. and Morton, J. (1991), "The impact resistance of composite materials-a review", *Compos.*, **22**(5), 347-362.

Cevik, M. (2010), "In-plane vibration analysis of symmetric angle-ply laminated composite arches", *Gazi Univ. J. Sci.*, **23**(2), 187-199.

Chen, W.Q., Lv, C.F. and Bian, Z.G. (2003), "Elasticity solution for free vibration of laminated beams", *Compos. Struct.*, **62**, 75-82.

Choi, H.Y. and Chang, F. A. (1991), "New approach toward understanding damage mechanisms and mechanics of laminated composites due to low-velocity impact", *J. Compos. Mater.*, **25**, 992-1038.

Chun, K.S. and Kassegne, S.K. (2005), "Low-velocity impact dynamic behavior of laminated composite nonprismatic folded plate structures", *J. Eng. Mech.*, **131**(7), 678-688.
Cunedioglu, Y. (2011), "Analyses of Laminated Cantilever Composite Beams by Model Order Reduction Techniques", *Mech. Base. Des. Struct.*, **39**, 22-45.
Harris, C. (2002), *Harris' shock and vibration handbook*, 5th Edition, McGraw-Hill, USA.
Kaw, A.K. (2006), *Mechanics of composite materials*, 2nd Edition, Taylor Francis, London.
Kiral, B.G. (2009), "Free vibration analysis of delaminated composite beams", *Sci. Eng. Compos. Mater.*, **16**(3), 209-224.
Kisa, M. (2004), "Free vibration analysis of a cantilever composite beam with multiple cracks", *Compos. Sci. Technol.*, **64**, 1391-1402.
Kumar, J.S., Raju, D. and Reddy, K.V.K. (2011), "Vibration analysis of composite laminated plates under higher order shear deformation theory with zig-zag function", *Ind. J. Sci. Technol.*, **4**(8), 960-966.
Lagace, P.A. and Wolf, E. (1993), "Impact damage resistance of several laminated material systems", *Proceedings of the Structural Dynamics and Materials Conference*, 1863-1872.
Numayr, K.S., Haddad, M.A. and Ayoub, A.F. (2006), "Investigation of free vibrations of composite beams by using the finite-difference method", *Mech. Compos. Mater.*, **42**(3), 231-242.
Reddy, J.N. (1992), *Finite element analysis of composite laminates*,1st Edition, Springer.
Setoodeh, A.R., Malekzadeh, P. and Nikbin, K. (2009), "Low-velocity impact analysis of laminated composite plates using a 3D elasticity based layer-wise FEM", *Mater. Des.*, **30**, 3795-3801.
Sun, C.T. and Chen, J.K. (1985), "On the impact of initially stressed composite laminates", *J. Comput. Math.*, **19**(11), 490-504.
Tiberkak, R., Bachene, M., Rechak, S. and Necib, B. (2008), "Damage prediction in composite plates subjected to low-velocity impact", *Compos. Struct.*, **83**, 73-82.
Yildirim, V. and Kiral, E. (2000), "Investigation of the rotary inertia and shear deformation effects on the out-of-plane bending and torsional natural frequencies of laminated beams", *Compos. Struct.*, **49**, 313-320.

CC